TRAPPING OF WAVES BY THIN FLOATING ICE SHEETS

by R. PORTER

(*School of Mathematics, University of Bristol, Bristol, BS8 1TW, UK.*)

Summary

It is shown that localised wave motions (often referred to edge waves or trapped modes) are capable of being supported by two complementary arrangements involving floating ice on water: a finite width ice sheet of constant thickness floating on open water; and an open water channel – or lead – embedded in an ice-covered ocean. The search for such solutions is motivated by a simple observation, evidently not made before, that wavelengths of propagating waves in thin ice sheets can be either greater or less than those of the same frequency on an unloaded water surface depending on physical parameters in the problem. The existence of edge waves are confirmed by accurate computations of solutions to integral equations derived from the underlying boundary-value problems using Fourier transform methods.

1. Introduction

The interaction between ocean waves and thin floating elastic plates has been the subject of a large number of papers in recent years, with the principal application area being the study of sea ice. Its practical importance is in furthering the understanding of wave energy propagation within the Marginal Ice Zone, an area of broken floating ice floes between the open ocean and the shore-fast sea ice. In particular, the dependence of sea ice and prevailing ocean wave conditions in assisting the further break-up of ice sheets is a poorly-understood process but one which plays an important part in climate modelling, (**1**). An informative review can be found in (**2**).

Statistical studies (e.g. (**3**), (**4**), (**5**)) of wave propagation through broken sea ice use information taken from fundamental ocean wave/sea ice interaction problems. These include determining how energy is transferred from ocean waves to flexural-gravity waves across the edge of an ice sheet (e.g. (**6**), (**7**), (**8**)); or how waves propagate across narrow cracks, 'ridges' and 'keels' in ice sheets (e.g. (**9**), (**10**), (**11**), (**12**)) across open water 'leads' between ice sheets (**13**), or across ice sheets of finite extent (e.g. (**14**), (**15**)). More complicated problems involve determining fully three-dimensional scattering characteristics from finite ice floes (**16**), (**17**) to their interaction effects in large arrays (**18**), (**19**).

All problems listed above assume the existence of an incoming wave field and measure some effects of practical importance. However it can also be important to consider situations in which there is no incoming source of wave energy. Instead wave energy is assumed to be confined within the particular arrangement of ice sheet and open water and it is this aspect of wave/ice sheet interaction with which our concern rests here. To highlight its significance, in mechanical systems the analogue of such a study would be to identify structural resonances. For examples of the influence of 'wave trapping' on water wave problems in related contexts, see (**20**). In the context of ice sheets knowledge of localised solutions is important in determining solutions to certain types of inhomogeneous problems; see for e.g. (**21**).

 © Oxford University Press ????

We will consider two specific arrangements of thin floating ice sheets. The first involves an ice sheet of constant finite width and infinite length; the second is the complementary arrangement in which a open water channel of constant width (i.e. a lead) is embedded between two semi-infinite ice sheets. In both cases the fluid will be assumed, for simplicity, to be of infinite depth.

In the first case we consider the existence of flexural-gravity waves trapped within the ice sheet; that is, their energy is not able to radiate away from the ice sheet in the form of ocean surface waves. For reasons which will be explained later within the paper, this problem turns out to be simpler to construct solutions to than the second. There, we consider surface waves trapped within the open water lead between the two ice sheets in which energy is not able to radiate to infinity through the ice sheet in the form of flexural-gravity waves.

Both types of solution described above are generically referred to as 'trapped waves' in the water wave literature. Because of the particular class of solution that they represent, they are also often referred to as 'edge waves'. This terminology originates from Stokes (**22**) who determined an explicit solution wave motion localised to the edge of a plane beach. Many examples have since emerged of edge waves in a variety of settings. The generic description is a geometry which is constant in one horizontal (longshore) direction, allowing a wave-like behaviour to be assumed in that direction; this has the mathematical effect of reducing a three-dimensional boundary-value problem to one posed in a two-dimensional cross-sectional plane. If the wavenumber describing the longshore wave behaviour is assumed to be greater than the wavenumber of free waves at infinity then, by construction, radiation of energy to infinity is prohibited and any non-trivial solution of the reduced two-dimensional problem would describe edge waves. This is neither a necessary or sufficient condition for the existence of edge waves.

Applying the reasoning above in the context of ice sheets (**23**), (**10**) and (**24**) showed that edge waves could be supported by an infinitely-narrow crack between two adjacent ice sheets floating on water. These are peculiar results in the sense that they do not follow the standard reasoning described below. They perhaps are more closely related to edge waves that are known to exist along thin elastic plates without fluid loading, (**25**).

The usual heursitic argument that motivates the existence of edge waves are an extension of those already introduced. Assume the wavenumber is k_- at $x = -\infty$ and at $x = +\infty$ it is $k_+ > k_-$, say. Waves propagating from $x = +\infty$ at an oblique angle θ_+ will possess a longshore component of wavenumber $l = k_+ \sin\theta_+$. For θ_+ above some critical angle l becomes greater than k_- implying no waves can propagate to $x = -\infty$. In simple physical terms an oblique wave undergoes total internal reflection at the interface between domains with different phase speeds. If two such interfaces are reflected about an origin so that the wavenumber tends to k_- at both $x = \pm\infty$ but rises to $k_+ > k_-$ at the origin then oblique waves will undergo persistent reflections and become trapped.

It is this mechanism which underpins the present study. Motion of angular frequency ω is assumed. Waves on the surface of the fluid have a wavenumber $K = \omega^2/g$ where g is gravitational acceleration. Flexural-gravity waves supported by a floating elastic plate are characterised by a positive real wavenumber κ which is known to satisfy the relation (see, for example, (**9**))

$$(\beta\kappa^4 + 1 - K\delta)\kappa - K = 0. \tag{1}$$

Here β and δ are positive parameters which encode properties of the elastic plate and

the fluid. The existence of a positive real root of (1) can be established by considering intersection of the graphs of the functions $f(\kappa) = (\beta\kappa^4 - K\delta)\kappa$ and $K - \kappa$. In particular, one can then readily determine that $\kappa < K$ if $K > K^*$ where $K^* = (\delta/\beta)^{1/3}$ and, conversely, that $\kappa > K$ if $K < K^*$.

In other words, depending on wave frequency and parameters of the elastic plate, wavenumbers of free waves in the elastic plate can be either greater than or less than the wavenumber of those on the ocean. According to the arguments rehearsed earlier, if $\kappa > K$ we will expect total internal reflection to occur as waves move from ice to water and vice versa if $\kappa < K$.

This provides the evidence of the existence of trapped waves in ice sheets and open water leads. In Sections 2 and 3 we calculate these edge waves using Fourier transform methods before the work is summarised in §4. In the first of two appendices we include details associated with the solution to one of the problems and provide details of conditions needed to calculate edge waves along cracks in the second.

2. Trapped waves in a floating ice sheet of finite width

Cartesian coordinates are used with $z = 0$ coinciding with the undisturbed surface of a fluid of density ρ_w and z pointing upwards. A scaling of coordinates is assumed such that the elastic plate lies between $-1 < x < 1$, $z = 0$, for all y. Classical linearised water wave theory is used in which the velocity potential used to describe the fluid motion can be written

$$\Phi(x, y, z, t) = \Re\{\phi(x, z)\mathrm{e}^{\mathrm{i}ly}\mathrm{e}^{-\mathrm{i}\omega t}\}. \tag{2}$$

Thus, a dimensionless 'longshore' wavenumber l and a single frequency time dependence $\omega/2\pi$ are assumed and it follows that the complex-valued reduced potential $\phi(x, z)$ satisfies

$$(\nabla^2 - l^2)\phi = 0, \qquad \text{in } z < 0,\ -\infty < x < \infty \tag{3}$$

where $\nabla = (\partial_x, \partial_z)$. In regions of open water the linearised kinematic and dynamic conditions on the free surface of the fluid combine to give the boundary condition

$$\phi_z - K\phi = 0, \qquad \text{on } z = 0 \tag{4}$$

where $K = \omega^2/g$. As $z \to -\infty$, $|\nabla\phi| \to 0$.

The ice sheet plate has density ρ_p, non-dimensional thickness $d \ll 1$ and is assumed to have negligible draft. Its deflection is modelled by Kirchhoff-Love thin elastic plate theory. Consequently regions of the surface covered by ice are represented by the boundary condition (e.g. see (**10**))

$$\left(\beta(\partial_x^2 - l^2)^2 + 1 - K\delta\right)\phi_z - K\phi = 0, \qquad \text{on } z = 0 \tag{5}$$

where $\beta = Ed^3/(12\rho_w g(1-\nu^2))$, $\delta = d(\rho_p/\rho_w)$ represent bending stiffness and heave inertia in terms of Young's modulus E and Poisson's ratio, ν. In addition, the edges of the plate must be free of bending moments and shear stress and this requires

$$(\partial_x^2 - \nu l^2)\phi_z = 0, \qquad \text{at } x = \pm 1,\ z = 0 \tag{6}$$

and

$$(\partial_x^3 - (2-\nu)l^2\partial_x)\phi_z = 0, \qquad \text{at } x = \pm 1,\ z = 0 \tag{7}$$

to hold. Note that both conditions must be applied in the limit as $x = \pm 1$ is approached from within the ice sheet region since ϕ_z, which represents elevation of the surface, is discontinuous across $x = \pm 1$.

Following the arguments presented in the Introduction we assume $l > K$ and $K < K^*$. This implies travelling waves are supported by the floating ice sheet but that waves cannot propagate to infinity on the ocean surface.

Clearly, we could decompose the boundary-value problem outlined above into a pair of problems which are symmetric and antisymmetric about the centreline $x = 0$ from the outset (as in (**10**) for example) – this is done in §3. Here, it is simpler to retain generality at this stage and identify symmetric and antisymmetric components towards the end of the solution.

Thus we define a Fourier transform

$$\overline{\phi}(\alpha, z) = \int_{-\infty}^{\infty} \phi(x, z) \mathrm{e}^{-\mathrm{i}\alpha x}\, dx \tag{8}$$

so that (3) is reduced to

$$\left(\frac{d^2}{dz^2} - \gamma^2\right) \overline{\phi} = 0 \tag{9}$$

where $\gamma = \sqrt{\alpha^2 + l^2}$. It follows that $\overline{\phi}(\alpha, 0) = A(\alpha)\mathrm{e}^{\gamma z}$. Taking the Fourier transforms of $\phi_z - K\phi$ on $z = 0$ and using (4) for $|x| > 1$ and (5) for $|x| < 1$ gives

$$(\gamma - K)A(\alpha) = \int_{-1}^{1} (K\delta - \beta(\partial_x^2 - l^2)^2)\phi_z(x, 0)\mathrm{e}^{-\mathrm{i}\alpha x}\, dx. \tag{10}$$

Inverting the transform gives

$$\phi(x, z) = \frac{1}{2\pi} \int_{-\infty}^{\infty} \frac{\mathrm{e}^{\gamma z}\mathrm{e}^{\mathrm{i}\alpha x}}{\gamma - K} \int_{-1}^{1} (K\delta - \beta(\partial_x^2 - l^2)^2)\phi_z(x', z)\mathrm{e}^{-\mathrm{i}\alpha x'}\, dx'\, d\alpha. \tag{11}$$

To derive an integral equation we either can apply the plate condition (5) to the left-hand side of (11) from which emerges a homogeneous first-kind integral equation. More simply, we can take a z-derivative of (11) and set $z = 0$ to obtain a second-kind integral equation

$$\phi_z(x, 0) = \frac{1}{2\pi} \int_{-\infty}^{\infty} \frac{\gamma\mathrm{e}^{\mathrm{i}\alpha x}}{\gamma - K} \int_{-1}^{1} (K\delta - \beta(\partial_x^2 - l^2)^2)\phi_z(x', 0)\mathrm{e}^{-\mathrm{i}\alpha x'}\, dx'\, d\alpha \tag{12}$$

over $|x| < 1$. Solutions of (12) also need to satisfy (6) and (7).

One could integrate by parts four times in (12) to transfer the four derivatives in x away from $\phi_z(x, 0)$, using (6) and (7) to simplify end point evaluations released from integration by parts. In doing so four auxiliarly unknowns appear in the solution, being the pointwise evaluations of displacement and gradients $\phi_z(\pm 1^{\mp}, 0)$, $\phi_{zx}(\pm 1^{\mp}, 0)$ at the edges of the ice sheets. This course of action is necesssary in §3 but makes the solution more complicated than is necessary here.

Instead solutions of (12) are sought by expanding $\phi_z(x, 0)$ as

$$\phi_z(x, 0) = \sum_{n=0}^{\infty} \frac{a_n w_n(x)}{K\delta - \beta k_n^4} \tag{13}$$

where $w_n(x)$ are eigenfunctions and k_n^4 play the part of the eigenvalues in the following homogeneous problem

$$\left(\frac{d^2}{dx^2} - l^2\right)^2 w_n(x) = k_n^4 w_n(x), \qquad |x| < 1 \tag{14}$$

with

$$w_n''(\pm 1) - \nu l^2 w_n(\pm 1) = 0, \qquad \text{and} \qquad w_n'''(\pm 1) - (2-\nu) l^2 w_n'(\pm 1) = 0. \tag{15}$$

This definition serves two purposes. It ensures that the solution satisfies (6) and (7) and, secondly, it converts derivatives embedded in (12) into multiplicative terms which can subsequently be factored from the integral. In (13) we have used the eigenmodes for oblique waves in an elastic plate without fluid loading in the series expansion for the unknown, a trick first employed in this context by (**26**).

The eigensolutions are determined in Appendix A where it is also shown that $w_n(t)$ are orthogonal and that

$$W_n(\sigma) = \int_{-1}^{1} w_n(x) \mathrm{e}^{-\mathrm{i}\sigma x}\, dx \tag{16}$$

can be determined explicitly; see (A16), (A17). Using (13) in (12), multiplying through by $w_m(x)$ and integrating over $|x| < 1$ leads to the infinite system of equations

$$\frac{a_m C_m^2}{(K\delta - \beta k_m^4)} - \sum_{n=0}^{\infty} a_n K_{mn} = 0, \qquad m = 0, 1, 2, \ldots \tag{17}$$

where C_m^2 are defined in Appendix A and

$$K_{mn} = \frac{1}{2\pi} \int_{-\infty}^{\infty} \frac{\sqrt{\alpha^2 + l^2}}{\sqrt{\alpha^2 + l^2} - K} W_n(\alpha) W_m(-\alpha)\, dt. \tag{18}$$

It is also shown in Appendix A that W_{2n} are even functions and W_{2n+1} are odd functions and it follows that (17) decouples into two systems of equations

$$\frac{a_{2m+\mu} C_{2m+\mu}^2}{(K\delta - \beta k_{2m+\mu}^4)} - \sum_{n=0}^{\infty} a_{2n+\mu} K_{2m+\mu,2n+\mu} = 0, \qquad m = 0, 1, 2, \ldots \tag{19}$$

for $\mu = 0, 1$ (even/odd respectively) where

$$K_{2m+\mu,2n+\mu} = \frac{(-1)^\mu}{\pi} \int_0^{\infty} \frac{\sqrt{\alpha^2 + l^2}}{\sqrt{\alpha^2 + l^2} - K} W_{2n+\mu}(\alpha) W_{2m+\mu}(\alpha)\, d\alpha. \tag{20}$$

Values of $\mu = 0, 1$ correspond to symmetric and antisymmetric edge wave solutions respectively.

2.1 *Results*

Numerically, we truncate the real symmetric equations (19) and search parameter space for non-trivial solutions. Typically, we have four decimal place accuracy for a system truncated to five terms. There are no poles in the integrals defining K_{mn} since $l > K$; returning to

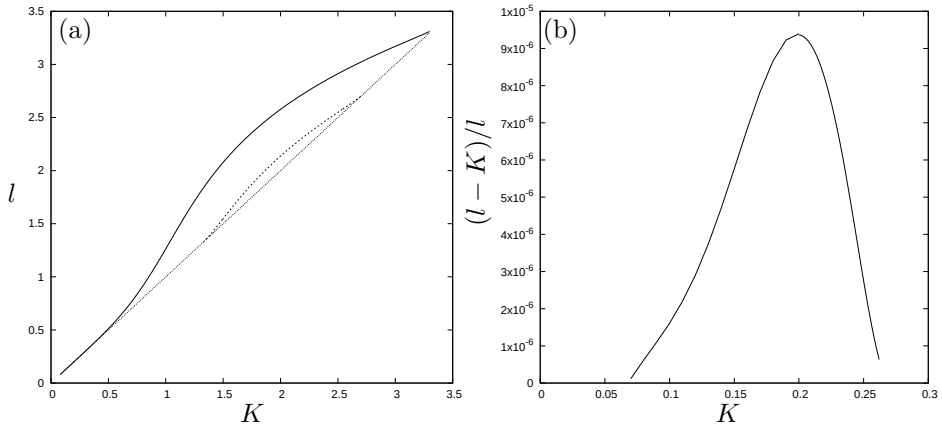

Fig. 1 In (a) symmetric (solid) and antisymmetric (dashed) edge wave relations between l and K; solutions exist above the cut-on $l = K$ (dotted) and for $K < K^* \approx 3.302$. Here, $\delta = 0.36$, $\beta = 0.01$, $\nu = 0.3$. In (b) the symmetric edge wave dispersion relation is visualised for $\delta = 0.09$, $\beta = 5$, $\nu = 0.3$ where $K^* \approx 0.262$.

(11) this condition confirms that the solution tends to zero as $|x| \to \infty$. The integrands in (20) decay like $O(\alpha^{-2})$ and the indefinite integrals approximated by truncation. For the accuracy required, this is done at $\alpha = 400$. We increase the truncation sizes of the system of equations and the accuracy of the numerical integration when higher accuracy is required.

Fig. 1 illustrates results found using the method outlined above. In order to illustrate results for both symmetric and antisymmetric trapped modes we have set parameters $\delta = 0.36$, $\nu = 0.3$ and $\beta = 0.01$ in Fig. 1(a). These parameters are not indicative of sea ice. They can be interpreted as an elastic sheet of thickness 1m and overall length 5m with $\rho_p/\rho_w = 0.9$, $\rho_w = 1025\text{kgm}^{-3}$ and a Young's modulus $E = 42891\text{Pa}$. In this example the elastic sheet is much more flexible than ice, whose Young's modulus is cited in the literature at a value of around $E = 6 \times 10^9\text{Pa}$. The solid and dashed curves provide the relation between frequency parameter, K, and longshore wavenumber, l, for symmetric and antisymmetric modes. We observe that the symmetric mode appears exists over the entire range $0 < K < K^*$ whilst the antisymmetric mode is cut-on across line $l = K$ within a sub-interval of the full range of K. As β increases the antisymmetric mode disappears across $l = K$ whilst symmetric mode results tend quickly towards the line $l = K$. Results using parameters corresponding to a realistic ice sheet are shown in Fig. 1(b) thickess 1m and width 20m where we have $\delta = 0.09$ and $\beta = 5$ are shown in Fig. 1(b). It can be seen values of l corresponding to a single symmetric edge wave lie in close proximity to K across a range of frequencies up to $K^* \approx 0.262$. Although this mode appears to vanish across the line $l = K$ at a frequency away from the origin it is believed that this is caused by a lack of numerical resolution (computations accurate to over 10 decimal places are required to resolve that level of detail).

In practical terms, with l and K being so close to each other, edge waves in sea ice would not be detected. However, their existence would have to be taken into account if addressing problems of non-planar wave sources in the presence of a finite width plate.

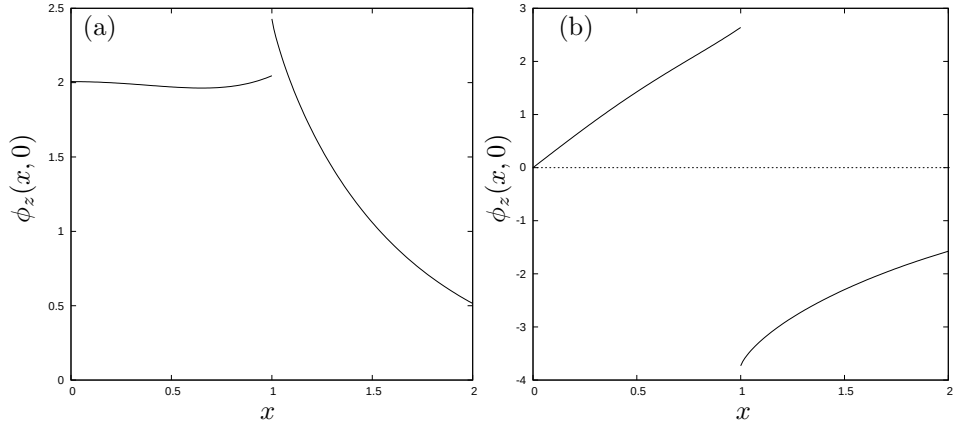

Fig. 2 Representation of the elevation of an elastic plate ($x < 1$) and water surface ($x > 1$) for (a) symmetric and (b) antisymmetric edge wave modes. Solutions correspond to $\delta = 0.36$, $\beta = 0.01$ and $l = 2$ with $K = 1.44077$ in (a) and $K = 1.86455$ in (b).

In Fig. 2 the motions of symmetric and antisymmetric edge waves are represented for the parameters computed in Fig. 1(a). The graphs represent amplitudes which are modulated in time and in the z-direction according to (2) and should be reflected about $x = 0$ appropriately. They obviously show the discontinuity in the displacements between the edge of the ice sheet and the water surface and the decay to zero in the displacement as $x \to \infty$.

3. Trapped waves in an open water lead between two ice sheets

This section concerns the same class of problem as in §2 but the intervals over which the two boundary conditions (4) and (5) hold are interchanged. The assumption made now is that $\kappa < l < K$ where κ satisfies (1) and that $K > K^* = (\delta/\beta)^{1/3}$. Following the arguments made in the Introduction, this choice prohibits wave radiation to infinity in the ice sheet, but allows travelling waves across the open water channel between the ice sheets.

The solution method here is more complicated than in §2 due to the interchange of boundary conditions. This is because the integral equation which will be derived below will apply to the solution across the lead between the ice sheets whilst edge conditions must be applied from a representation of the solution which holds across the ice sheet. Previously, the integral equation and edge conditions employed the same representation of the solution. We shall see how this complication emerges below. It also now turns out to be easier to decompose from the outset the problem into components symmetric and antisymmetric about the centreplane $x = 0$. We describe the symmetric solution in some detail and note the adjustments needed for the antisymmetric solution later.

3.1 *Symmetric edge wave solution*

We replace (8) with the definition

$$\overline{\phi}(\alpha, z) = \int_0^\infty \phi(x, z) \cos \alpha x \, dx. \tag{21}$$

Taking transforms of (3) gives the general solution $\overline{\phi}(\alpha,z)=A(\alpha)\mathrm{e}^{\gamma z}$ satisfying the deep water condition with $\gamma^2=\alpha^2+l^2$, as before. Our starting point is the identity

$$\int_1^\infty \big((\beta(\partial_x^2-l^2)^2+1-K\delta)\phi_z-K\phi\big)\cos\alpha x\,dx=0 \tag{22}$$

which hold on account of the elastic plate condition (5), now applied over $x>1$. Successively integrating by parts results in

$$(\beta\gamma^4+1-K\delta)\overline{\phi}_z(\alpha,0)-K\overline{\phi}(\alpha,0)+f_1(\alpha)\phi_{xz}(1^+,0)+f_2(\alpha)\phi_z(1^+,0)$$
$$=(\beta\gamma^4-K\delta)\int_0^1\phi_z(x',0)\cos\alpha x'\,dx' \tag{23}$$

in which the right-hand side has been simplified following use of free surface condition (4) in $0<x<1$. In the equation above we have defined functions

$$f_1(\alpha)=\beta(\alpha^2+\nu l^2)\cos\alpha,\qquad f_2(\alpha)=\beta(\alpha^3+(2-\nu)l^2\alpha)\sin\alpha. \tag{24}$$

Using $\overline{\phi}(\alpha,0)=A(\alpha)\mathrm{e}^{\gamma z}$ in (23) to solve for $A(\alpha)$ and inverting the transform gives

$$\phi(x,z)=\frac{2}{\pi}\int_0^\infty\frac{\mathrm{e}^{\gamma z}\cos\alpha x}{\Delta(\alpha)}\Big\{-f_1(\alpha)\phi_{xz}(1^+,0)-f_2(\alpha)\phi_z(1^+,0)$$
$$+(\beta\gamma^4-K\delta)\int_0^1\phi_z(x',0)\cos\alpha x'\,dx'\Big\}d\alpha \tag{25}$$

where

$$\Delta(\alpha)=(\beta\gamma^4+1-K\delta)\gamma-K. \tag{26}$$

This expression does not vanish for real α since we have assumed the cut-off condition $\kappa<l$ holds where κ as defined in (1) and since $\gamma^2=\alpha^2+l^2$. Consequently, $\phi\to0$ as $x\to\infty$ as there are no poles in the integrand in (25).

We take the z-derivative of (25) and set $z=0$ to get

$$\phi_z(x,0)=-F_1(x)\phi_{xz}(1^+,0)-F_2(x)\phi_z(1^+,0)$$
$$+\frac{2}{\pi}\int_0^\infty\left(1+\frac{K-\gamma}{\Delta(\alpha)}\right)\cos\alpha x\int_0^1\phi_z(x',0)\cos\alpha x'\,dx'd\alpha \tag{27}$$

where

$$F_i(x)=\frac{2}{\pi}\int_0^\infty\frac{\gamma f_i(\alpha)}{\Delta(\alpha)}\cos\alpha x\,d\alpha. \tag{28}$$

Noting that, for $x,x'>0$,

$$\frac{2}{\pi}\int_0^\infty\cos\alpha x\cos\alpha x'\,d\alpha=\delta(x-x') \tag{29}$$

we can write (27) as

$$-F_1(x)\phi_{xz}(1^+,0)-F_2(x)\phi_z(1^+,0)+\frac{2}{\pi}\int_0^\infty\frac{K-\gamma}{\Delta(\alpha)}\cos\alpha x\int_0^1\phi_z(x',0)\cos\alpha x'\,dx'd\alpha$$
$$=\begin{cases}\phi_z(x,0), & x>1\\ 0, & 0<x<1.\end{cases} \tag{30}$$

Returning to (28) we have, explicitly,

$$F_1(x) = \frac{2\beta}{\pi}\int_0^\infty \frac{\gamma(\alpha^2+\nu l^2)\cos\alpha}{\Delta(\alpha)}\cos\alpha x\, d\alpha \tag{31}$$

convergent for all x. With more work involving the use of the integral identity

$$\int_0^\infty \frac{\sin\alpha X}{\alpha}\, d\alpha = \frac{\pi}{2}\mathrm{sgn}(X) \tag{32}$$

we can show that

$$F_2(x) = \frac{1}{2}\mathrm{sgn}(x+1) - \frac{1}{2}\mathrm{sgn}(x-1) + \frac{2}{\pi}\int_0^\infty \frac{(K+\gamma(K\delta-1-\beta(l^4+\nu l^2\alpha^2)))\sin\alpha}{\alpha\Delta(\alpha)}\cos\alpha x\, d\alpha. \tag{33}$$

This form exposes the source of further discontinuities in the solution, but also improves the convergence of the integral critical when, as below, further derivatives are taken.

To complete the formulation of the problem we also need to take the x-derivative of (30) in the interval $x > 1$ and this gives

$$\phi_{xz}(x,0) = -F_1'(x)\phi_{xz}(1^+,0) - F_2'(x)\phi_z(1^+,0) - \frac{2}{\pi}\int_0^\infty \frac{\alpha(K-\gamma)}{\Delta(\alpha)}\sin\alpha x\int_0^1 \phi_z(x',0)\cos\alpha x' dx' d\alpha. \tag{34}$$

To calculate $F_1'(x)$ and $F_2'(x)$ we follow the earlier calculation of $F_2(x)$ and find

$$F_1'(x) = -\frac{1}{2}\mathrm{sgn}(x+1) - \frac{1}{2}\mathrm{sgn}(x-1) - \frac{2}{\pi}\int_0^\infty \frac{(K+\gamma(K\delta-1-\beta(l^4+(2-\nu)l^2\alpha^2)))\cos\alpha}{\alpha\Delta(\alpha)}\sin\alpha x\, d\alpha \tag{35}$$

and, provided $x \neq 1$,

$$F_2'(x) = -\frac{2}{\pi}\int_0^\infty \frac{(K+\gamma(K\delta-1-\beta(l^4+\nu l^2\alpha^2)))\sin\alpha}{\Delta(\alpha)}\sin\alpha x\, d\alpha. \tag{36}$$

In this formulation, there is one unknown function $\phi_z(x,0)$ defined over $|x| < 1$ which encodes the vertical fluid velocity across the surface of the gap between the elastic plates, and two unknown values $\phi_z(1^+,0)$ and $\phi_{xz}(1^+,0)$ which represent the displacements and gradients of the edges of the elastic plate.

They are determined as follows. First using (30) for $0 < x < 1$ results in the following integral equation for $\phi_z(x,0)$ across the surface

$$0 = -F_1(x)\phi_{xz}(1^+,0) - F_2(x)\phi_z(1^+,0) + \frac{2}{\pi}\int_0^\infty \frac{K-\gamma}{\Delta(\alpha)}\cos\alpha x\int_0^1 \phi_z(x',0)\cos\alpha x'\, dx' d\alpha \tag{37}$$

for $x < 1$. Reusing (30) for $x > 1$ in the limit $x \to 1^+$ gives

$$\phi_z(1^+,0) = -F_1(1^+)\phi_{xz}(1^+,0) - F_2(1^+)\phi_z(1^+,0) + \frac{2}{\pi}\int_0^\infty \frac{K-\gamma}{\Delta(\alpha)}\cos\alpha \int_0^1 \phi_z(x',0)\cos\alpha x'\,dx'd\alpha \quad (38)$$

and taking (34) also in the limit $x \to 1^+$ gives

$$\phi_{xz}(1^+,0) = -F_1'(1^+)\phi_{xz}(1^+,0) - F_2'(1^+)\phi_z(1^+,0) - \frac{2}{\pi}\int_0^\infty \frac{\alpha(K-\gamma)}{\Delta(\alpha)}\sin\alpha \int_0^1 \phi_z(x',0)\cos\alpha x'\,dx'd\alpha. \quad (39)$$

We go further and let $R_1^s(x)$ and $R_2^s(x)$ satisfy

$$\int_0^\infty \frac{K-\gamma}{\Delta(\alpha)}\cos\alpha x \int_0^1 R_i^s(x')\cos\alpha x'\,dx'd\alpha = F_i(x), \qquad 0 < x < 1 \quad (40)$$

$(i = 1, 2)$. It follows that

$$\phi_z(x,0) = (\pi/2)(R_1^s(x)\phi_{xz}(1^+,0) + R_2^s(x)\phi_z(1^+,0)) \quad (41)$$

for $0 < x < 1$ satisfies (37). Using (41) in (38) and (39) then results in

$$\begin{pmatrix} 1 + F_1'(1^+) + \mathcal{S}_1R_1^s & F_2'(1^+) + \mathcal{S}_1R_2^s \\ F_1(1^+) - \mathcal{S}_2R_1^s & 1 + F_2(1^+) - \mathcal{S}_2R_2^s \end{pmatrix} \begin{pmatrix} \phi_{xz}(1^+,0) \\ \phi_z(1^+,0) \end{pmatrix} = 0 \quad (42)$$

where we have introduced the notation

$$\mathcal{S}_1R_i^s = \int_0^\infty \frac{\alpha(K-\gamma)}{\Delta(\alpha)}\sin\alpha \int_0^1 R_i^s(x')\cos\alpha x'\,dx'd\alpha \quad (43)$$

and

$$\mathcal{S}_2R_i^s = \int_0^\infty \frac{(K-\gamma)}{\Delta(\alpha)}\cos\alpha \int_0^1 R_i^s(x')\cos\alpha x'\,dx'd\alpha. \quad (44)$$

In other words edge waves correspond to the vanishing of the real determinant of the 2×2 system (42) given in terms of solutions of the forced equations (40).

3.2 *Numerical method*

We expand the unknown functions which encode the vertical fluid velocity across the water surface as

$$R_i(x) \approx \sum_{n=0}^{N} b_{2n}^{(i)} v_{2n}(x), \qquad |x| < 1 \quad (45)$$

and choose $v_{2n}(x) = (-1)^n P_{2n}(x)$ where $P_n(x)$ are Legendre functions. We note the relation (see (**27**))

$$\int_0^1 v_{2n}(x)\cos\alpha x\,dx = j_{2n}(\alpha) \quad (46)$$

where $j_n(\alpha)$ is a spherical Bessel function (e.g. $j_0(\alpha) = \sin\alpha/\alpha$) which decays like $1/\alpha$ as $\alpha \to \infty$. Note also that spherical Bessel functions can be expressed in terms of standard circular Bessel functions.

Using (45) in (40), multiplying by $v_{2m}(x)$ and integrating over $0 < x < 1$ gives

$$\sum_{n=0}^{\infty} b_{2n}^{(i)} M_{2m,2n} = F_{i,2m} \tag{47}$$

for $m = 0, 1, \ldots, N$ where

$$M_{2m,2n} = \int_0^\infty \frac{K-\gamma}{\Delta(\alpha)} j_{2m}(\alpha) j_{2n}(\alpha)\, d\alpha \tag{48}$$

with

$$F_{1,2m} = \frac{2}{\pi} \int_0^\infty \frac{\gamma\beta(\alpha^2 + \nu l^2)\cos\alpha}{\Delta(\alpha)} j_{2m}(\alpha)\, d\alpha \tag{49}$$

and

$$F_{2,2m} = \delta_{m0} + \frac{2}{\pi} \int_0^\infty \frac{(K + \gamma(K\delta - 1 - \beta(l^4 + \nu l^2\alpha^2)))\sin\alpha}{\alpha\Delta(\alpha)} j_{2m}(\alpha)\, d\alpha. \tag{50}$$

Infinite integrals are rapidly convergent and are approximated by truncation.

All we then require to complete the numerical solution is

$$\mathcal{S}_1 R_i^s \approx \sum_{n=0}^{N} b_{2n}^{(i)} \int_0^\infty \frac{\alpha(K-\gamma)}{\Delta(\alpha)} \sin\alpha j_{2n}(\alpha)\, d\alpha \tag{51}$$

and

$$\mathcal{S}_2 R_i^s \approx \sum_{n=0}^{N} b_{2n}^{(i)} \int_0^\infty \frac{K-\gamma}{\Delta(\alpha)} \cos\alpha j_{2n}(\alpha)\, d\alpha. \tag{52}$$

3.3 *Antisymmetric modes*

We follow a similar procedure for identifying antisymmetric modes by defining sine instead of cosine transforms. This leads to small algebraic differences to before and edge waves are now given by non-trivial solutions of

$$\begin{pmatrix} 1 + G_1'(1^+) - \mathcal{T}_1 R_1^a & G_2'(1^+) - \mathcal{T}_1 R_2^a \\ G_1(1^+) - \mathcal{T}_2 R_1^a & 1 + G_2(1^+) - \mathcal{T}_2 R_2^a \end{pmatrix} \begin{pmatrix} \phi_{xz}(1^+, 0) \\ \phi_z(1^+, 0) \end{pmatrix} = 0 \tag{53}$$

where

$$G_1(x) = \frac{2}{\pi} \int_0^\infty \frac{\beta\gamma(\alpha^2 + \nu l^2)\sin\alpha}{\Delta(\alpha)} \sin\alpha x\, d\alpha \tag{54}$$

$$G_2(x) = -\frac{1}{2}(\mathrm{sgn}(x+1) + \mathrm{sgn}(x-1)) - \frac{2}{\pi} \int_0^\infty \frac{K + \gamma(K\delta - 1 - \beta(l^4 + \nu l^2\alpha^2))}{\Delta(\alpha)} \frac{\cos\alpha}{\alpha} \sin\alpha x\, d\alpha \tag{55}$$

with

$$G_1'(1^+) = \frac{2}{\pi}\int_0^\infty \frac{K+\gamma(K\delta-1-\beta(l^4+(2-\nu)l^2\alpha^2))}{\Delta(\alpha)}\frac{\sin\alpha\cos\alpha}{\alpha}\,d\alpha \tag{56}$$

$$G_2'(1^+) = -\frac{2}{\pi}\int_0^\infty \frac{K+\gamma(K\delta-1-\beta(l^4+\nu l^2\alpha^2))}{\Delta(\alpha)}\cos^2\alpha\,d\alpha \tag{57}$$

and

$$\mathcal{T}_1 R_i^a = \int_0^\infty \frac{\alpha(K-\gamma)}{\Delta(\alpha)}\cos\alpha\int_0^1 R_i^a(x')\sin\alpha x'\,dx'd\alpha \tag{58}$$

$$\mathcal{T}_2 R_i^a = \int_0^\infty \frac{(K-\gamma)}{\Delta(\alpha)}\sin\alpha\int_0^1 R_i^a(x')\sin\alpha x'\,dx'd\alpha. \tag{59}$$

In the above $R_i^a(x)$ satisfy

$$\int_0^\infty \frac{(K-\gamma)}{\Delta(\alpha)}\sin\alpha x\int_0^1 R_i^a(x')\sin\alpha x'\,dx'd\alpha = G_i(x), \qquad 0<x<1 \tag{60}$$

for $i=1,2$.

Now we expand the unknown functions which encode the vertical fluid velocity across the water surface as

$$R_i^a(x) \approx \sum_{n=0}^N b_{2n+1}^{(i)} v_{2n+1}(x), \qquad |x|<1 \tag{61}$$

and choose $v_{2n+1}(x) = (-1)^n P_{2n+1}(x)$ such that

$$\int_0^1 v_{2n+1}(x)\sin\alpha x\,dx = j_{2n+1}(\alpha). \tag{62}$$

Using (61) in (60), multiplying by $v_{2m+1}(x)$ and integrating over $0<x<1$ gives

$$\sum_{n=0}^N b_{2n+1}^{(i)} M_{2m+1,2n+1} = F_{i,2m+1} \tag{63}$$

for $m=0,1,\ldots,N$ where

$$M_{2m+1,2n+1} = \int_0^\infty \frac{K-\gamma}{\Delta(\alpha)} j_{2m+1}(\alpha)j_{2n+1}(\alpha)\,d\alpha \tag{64}$$

with

$$F_{1,2m+1} = \frac{2}{\pi}\int_0^\infty \frac{\beta\gamma(\alpha^2+\nu l^2)\sin\alpha}{\Delta(\alpha)} j_{2m+1}(\alpha)\,d\alpha \tag{65}$$

and

$$F_{2,2m+1} = -\delta_{m0} - \frac{2}{\pi}\int_0^\infty \frac{K+\gamma(K\delta-1-\beta(l^4+\nu l^2\alpha^2))}{\Delta(\alpha)}\frac{\cos\alpha}{\alpha} j_{2m+1}(\alpha)\,d\alpha \tag{66}$$

whose integrand is bounded since the limit $j_{2m+1}(\alpha)/\alpha$ as $\alpha\to 0$ is bounded. Finally

$$\mathcal{T}_1 R_i^a \approx \sum_{n=0}^N b_{2n+1}^{(i)}\int_0^\infty \frac{\alpha(K-\gamma)}{\Delta(\alpha)}\cos\alpha j_{2n+1}(\alpha)\,d\alpha \tag{67}$$

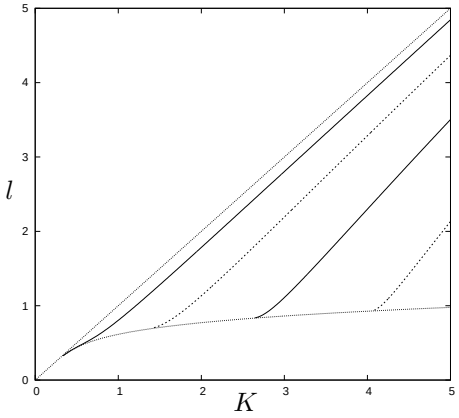

Fig. 3 Symmetric (solid) and antisymmetric (dashed) edge wave dispersion relations between l and K for an open water lead. Upper dotted curve is cut-off $l = K$ and lower dotted curve is cut-on $l = \kappa$. Here $\delta = 0.09$, $\beta = 5$, $\nu = 0.3$. The cut off/on curves meet at $K = K^* = (0.09/5)^{1/3} \approx 0.262$.

and

$$\mathcal{T}_2 R_i^a \approx \sum_{n=0}^{N} b_{2n+1}^{(i)} \int_0^\infty \frac{K-\gamma}{\Delta(\alpha)} \sin\alpha j_{2n+1}(\alpha)\, d\alpha. \tag{68}$$

3.4 *Results*

As in the previous section, numerical solutions are found by truncating infinite integrals at $\alpha = 400$ and choosing $N = 5$ in the solutions. In our calculations this was sufficient to claim four decimal place accuracy.

In Fig. 3 we present a typical example of the results found using the method described above. We have set $\delta = 0.09$ and $\beta = 5$ to represent 1m thick ice sheets bounding a lead 20m across. Fig. 3 shows the variation of dimensionless wavenumbers l against K corresponding to edge wave solutions computed using the methods outlined in the earlier part of this section. Solutions require $K > K^* = (\delta/\beta)^{1/3} \approx 0.262$ in this example and they lie in $\kappa < l < K$ where κ is given by (1). This range of values is depicted in Fig. 3 between the upper and lower dotted lines and to the right of their point of intersection. Using the scales employed in this example, $K = 1$ corresponds to $T \approx 6$s and $K = 4$, to $T \approx 3$s whilst $l = 1$ corresponds to a longshore wavelength approxmately 60m and $l = 4$ to roughly 15m. Taken together this is not an unrealistic set of parameters to encounter in a real sea ice environment.

In Fig. 4 a representation of the displacement of the water surface in the lead and the ice sheet beyond is given. Solutions are normalised by $\phi_z(1^+, 0)$. The parameters used are $\delta = 0.09$ and $\beta = 5$ giving $K^* \approx 0.262$. In both cases $l = 2$ is chosen and the first symmetric and antisymmetric modes are found to be at values $K = 2.2133$ and $K = 3.1168$ respectively. For larger values of β (which can be thought of as narrowing the lead) the contrast in displacement between the water in the lead and the ice sheet, which is already large in Fig. 4, being scaled to one hundredth of its computed size, increases.

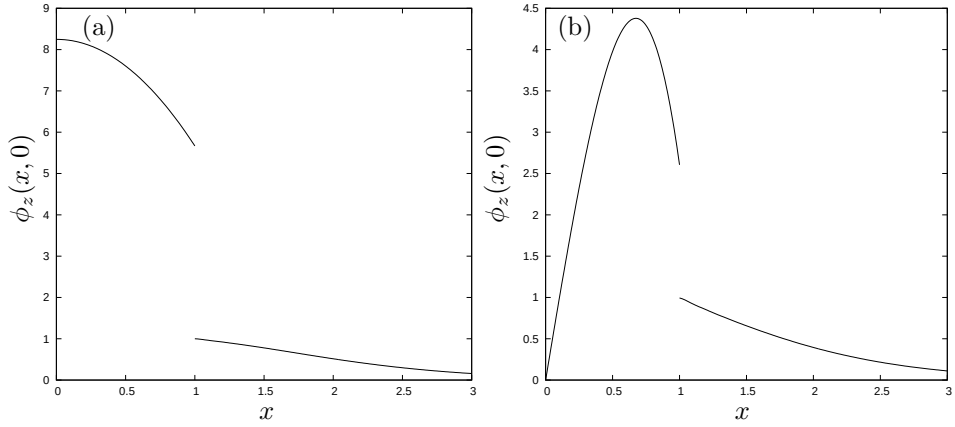

Fig. 4 Elevation of the water surface ($x < 1$) scaled to $\frac{1}{100}$th of its computed value and the ice sheet ($x > 1$) for (a) the symmetric and (b) the antisymmetric edge wave modes. Solutions correspond to $\delta = 0.09$, $\beta = 5$ and $l = 2$ with $K = 2.2133$ in (a) and $K = 3.1168$ in (b).

This last observation, namely that the narrowing of the lead results in a widening of the contrast between the surface displacements in the lead and on the ice sheet ties in with a separate mathematical observation. During the preparation of this paper a 'small-lead' approximation was attempted. Thus, one might expect edge wave solutions to tend to the infinitely-narrow crack solutions outlined in Appendix B as the size of lead is reduced. As it turns out the limit appears elusive. In that Appendix, there is a clue as to why this limit might not exist. In contrast to the finite lead problem outlined in §3, in the infinitely-narrow crack solution, one of the two conditions that the edge of the ice sheet satisfies is not applied during the construction of the solution through Fourier cosine or sine transforms. Instead, it is enforced on the solution afterwards.

4. Conclusions

In this paper it has been demonstrated that oblique flexural-gravity waves can be trapped in a long ice sheet of finite width floating on deep water. It has also been shown that oblique waves can be trapped in an open water lead between two semi-infinite floating ice sheets.

The calculation of edge wave solutions in both cases has involved the use of Fourier transforms to formulate integral equations over the finite interval occupied by either the ice sheet or the open water lead. The approach is not only simple to implement, it also has certain attractive features when compared to other candidate methods including those based on Green's functions, modified residue calculus and eigenfunction matching (e.g. (**16**), (**13**), (**14**)). For example, application of Green's functions result in singular integral equations and methods specific to finite depth result in having to find the roots of dispersion relations in addition to matching solutions along artificial boundaries. In this paper it is shown that expanding unknowns in the integral equations in an appropriate set of functions, the numerical solution is shown to converge rapidly.

The key to this work has been the observation from the ice dispersion relation (1), that wavelengths in ice sheets can be either greater or less than the corresponding wavelengths

for gravity waves on an uncovered ocean surface. This feature was exploited on a deep water assumption. It does, however, persist for all depths of fluid. For example, the shallow water (or long wave) ice-covered dispersion relation is

$$(\beta\kappa^4 + 1 - K\delta)\kappa^2 h - K = 0 \tag{69}$$

where h is the assumed small depth. Wavenumbers of propagating waves on water are defined by $k = \sqrt{K/h}$, say. Then it can be shown from (69) that $\kappa > k$ if $K < K^*$ and vice versa where, now, $K^* = \delta h^2/\beta$. That is, the critical wave frequency has a different dependence on δ and β than for deep water and one which includes fluid depth. By itself this guarantees the existence of shallow water edge wave solutions in both cases (ice sheet/lead) considered in this paper over all valid ranges of K.

The possibility of finding edge waves along the single straight edge of a semi-infinite floating ice sheet has also be investigated but it has been shown numerically that no such solutions exist.

References

1. Kohout, A.L., Williams, M.J.M., Dean, S.M. & Meylan, M.H. (2014) Storm-induced sea-ice breakup and the implications for ice extent. *Nature* **509**(7502) 604–607.

2. Squire, V.A. (2007) Of ocean waves and sea-ice revisited. *Cold Reg. Sci. Tech.* **49**(2) 110–133.

3. Williams, T.D., Bennetts, L.G., Squire, V.A., Dumont, D. & Bertino, L. (2013) Wave-ice interactions in the marginal ice zone. Part 1: Theoretical foundations. *Ocean Modelling* **71** 81–91.

4. Williams, T.D., Bennetts, L.G., Squire, V.A., Dumont, D. & Bertino, L. (2013) Wave-ice interactions in the marginal ice zone. Part 2: Numerical implementation and sensitivity studies along 1D transects of the ocean surface. *Ocean Modelling* **71** 92–101.

5. Montiel, F. Squire, V.A. & Bennetts, L.G. (2015) Reflection and transmission of ocean wave spectra by a band of randomly distributed ice floes. *Ann. Glaciol.* **56**(69) 315–322.

6. Tkacheva, L.A. (2001) Scattering of surface waves by the edge of a floating elastic plate. *J. Appl. Mech. Tech. Phys.* **42**(4) 638–646.

7. Linton, C.M. & Chung, H. (2003) Reflection and transmission at the ocean/sea-ice boundary. *Wave motion* **38**(1), 43–52.

8. Balmforth, N.J. & Craster, R.V. (1999) Ocean waves and ice sheets. *J. Fluid Mech.* **395**, 89–124.

9. Squire, V.A. & Dixon, A.W. (2001) How a region of cracked sea ice affects ice-coupled wave propagation. *Ann. Glaciol.* **33** , 327–332.

10. Evans, D.V. & Porter, R. (2003) Wave scattering by narrow cracks in ice sheets floating on water of finite depth. *J. Fluid Mech.* **484**, 143–165.

11. Williams, T.D. & Squire, V.A. (2006) Scattering of flexuralgravity waves at the boundaries between three floating sheets with applications. *J. Fluid Mech.* **569** 113–140.

12. Kohout, A.L. & Meylan, M.H. (2008) An elastic plate model for wave attenuation and ice floe breaking in the marginal ice zone. *J. Geophys. Res.* **113** (C9)

13. Chung, H. & Linton, C.M. (2005) Reflection and transmission across a finite gap in an infinite elastic plate on water. *Q.J. Mech. Appl. Math.* **58**, 1–15.
14. Kohout, A.L. & Meylan, M.H. (2006) A model for wave scattering in the marginal ice zone based on a two-dimensional floating-elastic-plate solution. *Ann. Glaciol.* **44**(1) 101–107.
15. Porter, D. & Porter, R (2004) Approximations to wave scattering by an ice sheet of variable thickness over undulating bed topography. *J. Fluid Mech.* **509** 145–179.
16. Meylan, M.H. (2002) Wave response of an ice floe of arbitrary geometry. *J. Geophys. Res.* **107** (C1).
17. Peter, M.A. & Meylan, M.H. (2004) Infinite-depth interaction theory for arbitrary floating bodies applied to wave forcing of ice floes. *J. Fluid Mech.* **500** 145–167.
18. Bennetts, L.G., Peter, M.A., Squire, V.A. & Meylan, M.H. (2010) A three-dimensional model of wave attenuation in the marginal ice zone. *J. Geophys. Res.* **115**(C12)
19. Bennetts L.G. & Williams T.D. (2015) Water wave transmission by an array of floating discs. *Proc. R. Soc. Lond. A* **471**:20140698.
20. Maniar, H. & Newman, J.N. (1997) Wave diffraction by long arrays of cylinders. *J. Fluid Mech.* **339** 309–330
21. Sturova, I.V. (2017) Action of a periodic surface pressure on an ice cover in the vicinity of a vertical wall. *J. Appl. Mech. Tech. Phys.* **58**(1) 80-88.
22. Stokes, G.G. (1846) Report on recent researches in hydrodynamics. *Rep. 16th meeting Brit. Assoc. Adv. Sci.* 1-20.
23. Marchenko, A.V. (1999) Parametric excitation of flexural-gravity edge waves in the fluid beneath an elastic ice sheet with a crack. *Eur. J. Mech. B/Fluids* **18** 511–525.
24. Williams, T.D. & Porter, R. (2009) The effect of submergence on the scattering by the interface between two semi-infinite sheets. *J. Fluids and Structures* **25**(5) 777–793.
25. Konenkov, Yu. K. (1960) A Rayleigh-type flexural wave. *Sov. Phys. Acoust.* **6** 122–123.
26. Newman, J.N. (1994) Wave effects on deformable bodies. *Appl. Ocean Res.* **16**(1) 47–59.
27. Porter, R. (2016) Surface wave interaction with rigid plates lying on water *Wave Motion* **66** 118–131.

APPENDIX A

The functions $w_n(x)$

In this section we derive solutions of the eigenproblem defined by

$$\left(\frac{d^2}{dx^2} - l^2\right)^2 w_n(x) = k_n^4 w_n(x), \qquad |x| < 1 \tag{A1}$$

with

$$w_n''(\pm 1) - \nu l^2 w_n(\pm 1) = 0, \qquad \text{and} \qquad w_n'''(\pm 1) - (2-\nu) l^2 w_n'(\pm 1) = 0 \tag{A2}$$

and calculate various quantities associated with those solutions. First, solutions to (A1) and (A2) which are *symmetric* about the origin are described by the functions

$$w_{2n}(x) = \frac{1}{4}\left(\frac{(k_{2n}^2 - (1-\nu)l^2)\cosh\sqrt{k_{2n}^2 + l^2}x}{(k_{2n}^2 + (1-\nu)l^2)\cosh\sqrt{k_{2n}^2 + l^2}} + \frac{\cos\sqrt{k_{2n}^2 - l^2}x}{\cos\sqrt{k_{2n}^2 - l^2}}\right) \tag{A3}$$

where k_{2n}^2 are defined as solutions of

$$(k_{2n}^2 + (1-\nu)l^2)^2\sqrt{k_{2n}^2 - l^2}\tan\sqrt{k_{2n}^2 - l^2} = -(k_{2n}^2 - (1-\nu)l^2)^2\sqrt{k_{2n}^2 + l^2}\tanh\sqrt{k_{2n}^2 + l^2}. \tag{A4}$$

Considering, first, the case where $k_{2n}^2 \geq l^2 > 0$, we solve for real positive values y of

$$-y\tan y = \frac{(y^2+\nu l^2)^2}{(y^2+(2-\nu)l^2)^2}\sqrt{y^2+2l^2}\tanh\sqrt{y^2+2l^2} \equiv f_s(y). \tag{A5}$$

Thus $f_s(0) = \nu^2 l\sqrt{2}\tanh(l\sqrt{2})/(2-\nu)^2$ and $f_s(y) \sim y$ as $y \to \infty$ and simple graphical considerations show that roots $y = y_n$ of (A5) lie in the ranges $(n-\frac{1}{2})\pi < y_n < n\pi$ for $n = 1, \ldots$ whilst $y_n \sim (n-\frac{1}{4})\pi$ as $n \to \infty$. It follows that $k_{2n}^2 = l^2 + y_n^2$ for $n = 1, \ldots$ define an infinite sequence of eigenvalue parameters.

Separately we need to consider the case $0 < k_{2n} < l$ where (A5) changes to

$$(k_{2n}^2+(1-\nu)l^2)^2\sqrt{l^2-k_{2n}^2}\tanh\sqrt{l^2-k_{2n}^2} = (k_{2n}^2-(1-\nu)l^2)^2\sqrt{k_{2n}^2+l^2}\tanh\sqrt{k_{2n}^2+l^2}. \tag{A6}$$

Graphical considerations can again be used to show that there is just one root k_0^2 lying between $(1-\nu)l^2$ and l^2. We note that $k_0 = 0$ when $l = 0$.

Eigenmodes which are *antisymmetric* about the origin are given by

$$w_{2n+1}(x) = \frac{1}{4}\left(\frac{(k_{2n+1}^2-(1-\nu)l^2)\sinh\sqrt{k_{2n+1}^2+l^2}x}{(k_{2n+1}^2+(1-\nu)l^2)\sinh\sqrt{k_{2n+1}^2+l^2}} + \frac{\sin\sqrt{k_{2n}^2-l^2}x}{\sin\sqrt{k_{2n+1}^2-l^2}}\right) \tag{A7}$$

where k_{2n+1}^2 are defined as solutions of

$$(k_{2n+1}^2+(1-\nu)l^2)^2\sqrt{k_{2n+1}^2-l^2}\cot\sqrt{k_{2n+1}^2-l^2} = (k_{2n+1}^2-(1-\nu)l^2)^2\sqrt{k_{2n+1}^2+l^2}\coth\sqrt{k_{2n+1}^2+l^2}. \tag{A8}$$

For $k_{2n+1}^2 > l^2$ we consider real positive values y satisfying

$$y\cot y = \frac{(y^2+\nu l^2)^2}{(y^2+(2-\nu)l^2)^2}\sqrt{y^2+2l^2}\coth\sqrt{y^2+2l^2} \equiv f_a(y). \tag{A9}$$

We see that the left-hand side tends to 1 as $y \to 0$ whilst $f_a(0) = \nu^2 l\sqrt{2}\coth(l\sqrt{2})/(2-\nu)^2$ and $f_a(y)$ is positive with $f_a(y) \sim y$ as $y \to \infty$. Graphical considerations now show that roots $y = y_n$ lie in $n\pi < y_n < (n+\frac{1}{2})\pi$ for $n = 1, \ldots$ whilst $y_n \sim (n+\frac{1}{4})\pi$ as $n \to \infty$. If $f_a(0) < 1$ then a root labelled y_0 exists in $(0, \pi/2)$. It follows that $k_{2n+1}^2 = l^2 + y_n^2$ over the range of values of n defined by the above arguments.

If $0 < k_{2n+1} < l$ then (A8) changes to

$$(k_{2n+1}^2+(1-\nu)l^2)^2\sqrt{l^2-k_{2n+1}^2}\coth\sqrt{l^2-k_{2n+1}^2} = (k_{2n+1}^2-(1-\nu)l^2)^2\sqrt{k_{2n+1}^2+l^2}\coth\sqrt{k_{2n+1}^2+l^2} \tag{A10}$$

Now graphical considerations can be used to show that there are no roots if $f_a(0) < 1$ and that if $f_a(0) > 1$ then there exists a single root which we can call k_1^2 and which lies between $(1-\nu)l^2$ and l^2. When $l = 0$, $k_1 = 0$. Thus k_1 is a root which is defined to be a solution of (A8) or (A10) depending on definitions of ν and l.

Eigenfunctions can be shown to be orthogonal by selecting eigenmodes and eigenvalues from either the symmetric ($\mu = 0$) or antisymmetric ($\mu = 1$) sets and considering

$$\begin{aligned}(k_{2n+\mu}^4 - k_{2m+\mu}^4)&\int_{-1}^{1} w_{2n+\mu}(x)w_{2m+\mu}(x)\,dx \\ &= \int_{-1}^{1}\left(\frac{d^2}{dx^2}-l^2\right)^2 w_{2n+\mu}(x)w_{2m+\mu}(x) - \left(\frac{d^2}{dx^2}-l^2\right)^2 w_{2m+\mu}(x)w_{2n+\mu}(x)\,dx = 0.\end{aligned} \tag{A11}$$

The final equality follows after integrating by parts twice and using the boundary conditions (A2). Since k_n are distinct in each symmetric and antisymmetric sets, it follows that

$$\int_{-1}^{1} w_{2n+\mu}(x)w_{2m+\mu}(x)\,dx = C^2_{2n+\mu}\delta_{mn} \tag{A12}$$

where C_n^2 are easy to calculate although result in messy expressions which are not obviously simplified. For completeness these turn out to be

$$C^2_{2n} = \frac{1}{16}\frac{(k_{2n}^2-(1-\nu)l^2)^2}{(k_{2n}^2+(1-\nu)l^2)^2}\tanh\sqrt{k_{2n}^2+l^2}\left[\frac{-2l^2}{(k_{2n}^2-l^2)\sqrt{k_{2n}^2+l^2}}+\right.$$
$$\left.\tanh\sqrt{k_{2n}^2+l^2}\left(-1+\frac{(k_{2n}^2+l^2)(k_{2n}^2-(1-\nu)l^2)^2}{(k_{2n}^2-l^2)(k_{2n}^2+(1-\nu)l^2)^2}\right)\right]+\frac{1}{16}\left[1+\frac{(k_{2n}^2-(1-\nu)l^2)^2}{(k_{2n}^2+(1-\nu)l^2)^2}\right]$$
$$+\frac{1}{8}\frac{(k_{2n}^2-(1-\nu)l^2)}{(k_{2n}^2+(1-\nu)l^2)}\left[\frac{\sqrt{k_{2n}^2+l^2}}{k_{2n}^2}\tanh\sqrt{k_{2n}^2+l^2}\right]\left[1-\frac{(k_{2n}^2-(1-\nu)l^2)^2}{(k_{2n}^2+(1-\nu)l^2)^2}\right] \tag{A13}$$

which can be used regardless of the sign of $k_{2n}^2-l^2$. The expression for C^2_{2n+1} is the same as (A13) above but with k_{2n} replaced by k_{2n+1} and tanh replaced by coth. In the case $l=0$, $C_0=1/2$, $C_1=1/6$ and $C_n=1/8$ for $n\geq 2$.

Next, from the definition (A1) we consider the identity

$$k_n^4\int_{-1}^{1} w_n(x)\mathrm{e}^{-\mathrm{i}\alpha x}\,dx = \int_{-1}^{1}\left(\frac{d^2}{dx^2}-l^2\right)^2 w_n(x)\mathrm{e}^{-\mathrm{i}\alpha x}\,dx \tag{A14}$$

and integrating by parts with the use of the boundary conditions (A2) we arrive at

$$(\gamma^4-k_n^4)\int_{-1}^{1} w_n(x)\mathrm{e}^{-\mathrm{i}\alpha x}\,dx = (\alpha^2+\nu l^2)\left[w_n'(x)\mathrm{e}^{-\mathrm{i}\alpha x}\right]_{-1}^{1}+\mathrm{i}(\alpha^3+(2-\nu)l^2\alpha)\left[w_n(x)\mathrm{e}^{-\mathrm{i}\alpha x}\right]_{-1}^{1} \tag{A15}$$

where $\gamma^2=\alpha^2+l^2$. Using the definition of $w_{2n}(x)$ in (A3) along with the relation (A4) we find

$$W_{2n}(\alpha)\equiv\int_{-1}^{1} w_n(x)\mathrm{e}^{-\mathrm{i}\alpha x}\,dx = \frac{k_{2n}^2}{(k_{2n}^2+(1-\nu)l^2)(\gamma^4-k_{2n}^4)}$$
$$\left[(\alpha^3+(2-\nu)l^2\alpha)\sin\alpha+\sqrt{k_{2n}^2+l^2}\tanh\sqrt{k_{2n}^2+l^2}\left(\frac{k_{2n}^2-(1-\nu)l^2}{k_{2n}^2+(1-\nu)l^2}\right)(\alpha^2+\nu l^2)\cos\alpha\right]. \tag{A16}$$

Likewise, when we use $w_{2n+1}(x)$ in (A7) we find

$$W_{2n+1}(\alpha)\equiv\int_{-1}^{1} w_{2n+1}(x)\mathrm{e}^{-\mathrm{i}\alpha x}\,dx = \frac{-\mathrm{i}k_{2n+1}^2}{(k_{2n+1}^2+(1-\nu)l^2)(\gamma^4-k_{2n+1}^4)}$$
$$\left[(\alpha^3+(2-\nu)l^2\alpha)\cos\alpha-\sqrt{k_{2n+1}^2+l^2}\coth\sqrt{k_{2n+1}^2+l^2}\left(\frac{k_{2n+1}^2-(1-\nu)l^2}{k_{2n+1}^2+(1-\nu)l^2}\right)(\alpha^2+\nu l^2)\sin\alpha\right]. \tag{A17}$$

APPENDIX B

Cracks

It is easy to rework the analysis of §3 in the case of an infinitely-thin crack (i.e. no lead) between two ice sheets. For symmetric edge wave solutions this leads to (27) being replaced by

$$\phi_z(x,0) = -\phi_{xz}(0^+,0)\left[\frac{2\beta}{\pi}\int_0^\infty \frac{\gamma(\alpha^2+\nu l^2)}{\Delta(\alpha)}\,d\alpha\right] \tag{B1}$$

Unlike the solution (27) considered in §3, this expression has been derived by applying just one of the two boundary conditions at the edge of the ice sheet. In order to apply the other, we need to take two further derivatives. First,

$$\phi_{xz}(x,0) = \phi_{xz}(0^+,0)\left[1+\frac{2}{\pi}\int_0^\infty \frac{K+\gamma(K\delta-1-\beta(l^4+(2-\nu)l^2\alpha)^2)}{\Delta(\alpha)}\frac{\sin\alpha x}{\alpha}\,d\alpha\right] \tag{B2}$$

for $x>0$ using the methods of §3, and then more straightforwardly,

$$\phi_{xxz}(x,0) = \phi_{xz}(0^+,0)\left[\frac{2}{\pi}\int_0^\infty \frac{K+\gamma(K\delta-1-\beta(l^4+(2-\nu)l^2\alpha^2))}{\Delta(\alpha)}\cos\alpha x\,d\alpha\right]. \tag{B3}$$

So imposing the final edge condition $\phi_{xxz}(0^+,0)-\nu l^2\phi_z(0^+,0)=0$ with (B1) and (B3) above gives

$$\int_0^\infty \frac{K+\gamma(K\delta-1-\beta(1-\nu)((1+\nu)l^4+2l^2\alpha^2))}{\Delta(\alpha)}\,d\alpha = 0 \tag{B4}$$

as the condition for a symmetric edge wave supported by an infinitely-thin crack.

In the case of antisymmetric edge wave solution in the presence of an infinitely-narrow crack we find, using Fourier sine transforms that

$$\begin{aligned}\phi_z(x,0) &= \phi_z(0^+,0)\left[\frac{2\beta}{\pi}\int_0^\infty \frac{\gamma(\alpha^4+(2-\nu)l^2\alpha)}{\Delta(\alpha)}\frac{\sin\alpha x}{\alpha}\,d\alpha\right]\\ &= \phi_z(0^+,0)\left[1+\frac{2}{\pi}\int_0^\infty \frac{K+\gamma(K\delta-1-\beta(l^4+\nu l^2\alpha^2))}{\Delta(\alpha)}\frac{\sin\alpha x}{\alpha}\,d\alpha\right]\end{aligned} \tag{B5}$$

for $x>0$. This expression has been derived without imposing the condition $\phi_{xxxz}(0^+,0)-\nu l^2\phi_{xz}(0^+,0)=0$ and to do this we first need

$$\phi_{xz}(x,0) = \phi_z(0^+,0)\left[\frac{2}{\pi}\int_0^\infty \frac{K+\gamma(K\delta-1-\beta(l^4+\nu l^2\alpha^2))}{\Delta(\alpha)}\cos\alpha x\,d\alpha\right] \tag{B6}$$

and then

$$\begin{aligned}\phi_{xxz}(x,0) &= \phi_z(0^+,0)\left[-\frac{2}{\pi}\int_0^\infty \frac{\alpha^2(K+\gamma(K\delta-1-\beta l^4))-\beta\gamma\nu l^2\alpha^4))}{\Delta(\alpha)}\frac{\sin\alpha x}{\alpha}\,d\alpha\right]\\ &= \phi_z(0^+,0)\left[\nu l^2-\frac{2}{\pi}\int_0^\infty \frac{(\alpha^2-\nu l^2)(K+\gamma(K\delta-1-\beta l^4))+2\beta\gamma\nu l^4\alpha^2}{\Delta(\alpha)}\frac{\sin\alpha x}{\alpha}\,d\alpha\right]\end{aligned} \tag{B7}$$

for $x>0$. Finally, another x-derivative gives us

$$\phi_{xxxz}(x,0) = \phi_z(0^+,0)\left[-\frac{2}{\pi}\int_0^\infty \frac{2\beta\gamma\nu l^4\alpha^2+(\alpha^2-\nu l^2)(K+\gamma(K\delta-1-\beta l^4))}{\Delta(\alpha)}\cos\alpha x\,d\alpha\right]. \tag{B8}$$

Using (B5) and (B7) into the condition $\phi_{xxxz}(0^+,0)-(2-\nu)l^2\phi_{xz}(0^+,0)=0$ results, after some work, in

$$\int_0^\infty \frac{(\alpha^2+2(1-\nu)l^2)(K+\gamma(K\delta-1-\beta l^4))+\nu^2\beta\gamma l^4\alpha^2}{\Delta(\alpha)}\,d\alpha = 0 \tag{B9}$$

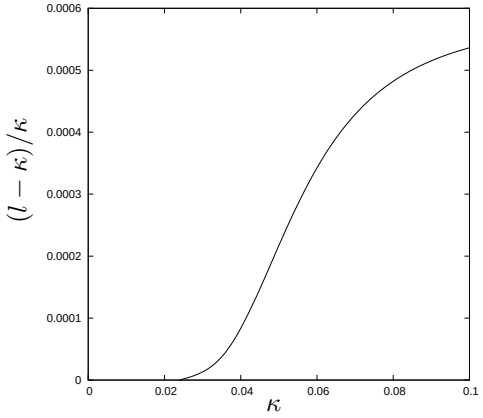

Fig. A Symmetric edge wave dispersion relations showing $(l-\kappa)/\kappa$ against κ for a narrow crack in deep water with $\delta = 0.9$, $\beta = 65535$ and $\nu = 0.3$.

as the condition to be satisfied for antisymmetric edge waves.

Computations of the symmetric condition confirm what was commented on in (**10**) and computed in (**24**) for finite water depth, which is that symmetric edge waves do exist for values of l fractionally above the cut-off value of κ, as defined in (1). A curve showing this relation for deep water using (B4) is shown in Fig. A, in which parameters corresponding to a 1m thick ice sheet are used. The condition for antisymmetric edge waves is never satisfied.